Can Temperature Extremes in East Antarctica be Replicated from ERA Interim Reanalysis?

Authors: Xie, Aihong, Wang, Shimeng, Xiao, Cunde, Kang, Shichang, Gong, Juanxiao, et al.

Source: Arctic, Antarctic, and Alpine Research, 48(4) : 603-621

Published By: Institute of Arctic and Alpine Research (INSTAAR), University of Colorado

URL: https://doi.org/10.1657/AAAR0015-048

Arctic, Antarctic, and Alpine Research, Vol. 48, No. 4, 2016, pp. 603–621
DOI: http://dx.doi.org/10.1657/AAAR0015-048

Can temperature extremes in East Antarctica be replicated from ERA Interim reanalysis?

Aihong Xie[1,*], Shimeng Wang[1,*], Cunde Xiao[1,2], Shichang Kang[1], Juanxiao Gong[1], Minghu Ding[2], Chuanjin Li[1], Tingfeng Dou[3], Jiawen Ren[1], and Dahe Qin[1]

[1]State Key Laboratory of Cryospheric Sciences, Northwest Institute of Eco-Environment and Resources, Chinese Academy of Sciences, Donggang West Road 320, Lanzhou, Gansu 730000, China
[2]Chinese Academy of Meteorological Sciences, Beijing 100081, China
[3]College of Resources and Environment, University of Chinese Academy of Sciences, Beijing 100049, China
[*]Corresponding authors' email addresses: (Xie) xieaih@lzb.ac.cn; (Wang) wangshimeng@lzb.ac.cn

A B S T R A C T

Based on daily minimum, maximum, and mean surface air temperatures (T_{min}, T_{max}, T_{mean}) from the European Centre for Medium-Range Weather Forecast's reanalysis from 1979 onwards (ERA Interim), the accuracy of daily T_{min} and T_{max} reanalysis is assessed against in situ observations from four automatic weather stations (Zhongshan, EAGLE, LGB69, and Dome A) in East Antarctica from 2005 to 2008. ERA Interim generally shows a warm bias for T_{min} and a cool bias for T_{max}, with an underestimation of the diurnal temperature range. The reanalysis explains more than 84% of the daily and annual variance, and the replicating ability decreases gradually from the coast to the interior, with annual root mean square errors of 2.4 °C, 2.6 °C, 3.0 °C, and 4.3 °C for daily T_{min}, and 2.2 °C, 3.1 °C, 3.4 °C, and 4.9 °C for daily T_{max} at Zhongshan, LGB69, Eagle, and Dome A, respectively. ERA Interim shows little seasonal variability, although it performs a little better in the austral spring and worse in winter and autumn at Dome A. An analysis on spatial distribution of temperature and wind field indicates that ERA Interim has successfully replicated the progress of temperature extremes developing, occurring, and disappearing. In addition, weather events extracted from ERA Interim mainly occur on the same day as observations, with high cross-correlation coefficients ($R \geqq 0.287$, $N \geqq 1131$, $P < 0.001$). ERA Interim has, despite its regional limitations and deficiencies, proved to be a powerful tool for weather and climate studies in the Antarctic region.

Introduction

In late December 2015, a powerful warm current suddenly drove the North Pole temperature back up to the freezing point, 50 °C above average for that time of year. Buoy measurements confirmed that anomalous temperatures climbed above 32 °C on 30 December. Subsequently, in late January 2016, an unprecedented cold snap occurred over East Asia, Southeast Asia, northern parts of South Asia, and northern North America, yielding the coldest temperatures in decades in many of these regions. The resulting snowfalls and frigid weather stranded thousands of people. If such temperature extremes occurred in Antarctica, there would be even greater worldwide effects, since Antarctica has much greater heat reserves. On the other hand, mass loss owing to sublimation and erosion of snow by the wind has a potentially large impact on the surface mass balance (van den Broeke et al., 1999), prolonged katabatic wind events affect the near-surface climate, summer melt percolation and changes in the stress field due to shelf removal play a major role in glacier dynamics, and extreme snowmelt events have

a great impact on ice shelf disintegration (Cape et al., 2015; Marshall and Thompson, 2016; Scambos et al., 2004; Shepherd et al., 2012).

Weather extremes are occurrences of weather with meteorological variable values above (or below) the upper (or lower) limit of observed threshold values. Their probability of occurrence is generally lower than 10%. Statistically, weather extremes are generally regarded as events of "low probability" (IPCC, 2012; Qin et al., 2015). New evidence has confirmed that climate change will affect the frequency, intensity, spatial extent, and duration of weather extremes (IPCC, 2012, 2013; Qin et al., 2015). To determine the direction and extent of changes in extreme weather, appropriate analytical methods and high-quality observational data homogenization are prerequisites. The infrequent occurrence of extreme events makes it difficult to identify their long-term changes, compared with identifying changes in average climatic conditions. In particular, analysis of changes in extreme weather events has higher requirements of observational data. To analyze the changes in extreme events at shorter time scales, high-resolution data collected daily or at even shorter time scales are required. This can be problematic, first because it is difficult to obtain data at high temporal resolution, and second because the quality of such observations may be insufficiently high (Qin et al., 2015). Specifically, meteorological records are spatially limited and of short duration in Antarctica for adequately characterizing its remote and harsh environment. Thus, there is little research on its extreme weather events (Kennicutt et al., 2014), making it a blank cell with regard to changes in the intensity and frequency of its extreme weather events (IPCC, 2013).

Reanalysis data provide a multivariate, spatially complete, and coherent record of global atmospheric circulation (Dee et al., 2011; Kalnay et al., 1996; Kistler et al., 2001). They place great emphasis on regenerating synoptic analyses over several decades, using a fixed data assimilation system and numerical weather prediction model (Compo et al., 2011). Despite the indisputable uncertainty of its data products, comparisons reveal broad agreement in the long-term trends of its temperature time series (Pezza et al., 2012; Simmons, 2004; Simmons et al., 2014), Hence, data sets generated by such reanalysis can be of great value for atmospheric research on climate anomalies (such as monthly and annual mean temperature) (Dee et al., 2011). Kharin et al. (2007) showed some substantial differences between extreme values derived from models versus observations. Donat et al. (2014) found a high level of consistency between various interpolated observations of temperature extremes over the past 60 years, with most reanalysis reproducing observed changes and spatial patterns reasonably well for the post-1979 period, when satellite data were available for assimilation. In Europe, Cornes and Jones (2013) demonstrated a good agreement between gridded observations and the reanalysis data over the past 30 years for extreme temperatures. Russo et al. (2014) used gridded data sets of in situ observations and reanalysis data to evaluate extreme temperatures in various simulations. They highlighted the large spread in absolute values of temperature extremes from different reanalysis products, comparable to the spread for different climate models. You et al. (2014) assessed the consistency and discrepancy in extreme indices between reanalysis and observations in China (You et al., 2014). They suggested that the European Centre for Medium-range Weather Forecasts (ECMWF) reanalysis can reproduce the variability of temperature extremes obtained from observations, and can be applied to investigate climate extremes to a limited extent, although they cautioned that biases exist because of assimilation differences.

Previous research in Antarctica has emphasized mean temperature (T_{mean}) from reanalysis and observations, showing that reanalysis data are useful for monitoring changes in data-sparse regions (Boccara et al., 2008; Bromwich et al., 2007; Genthon et al., 2010; Gobiet, 2005; Xie et al., 2014). Few studies in Antarctica have focused on maximum temperatures (T_{max}) or minimum temperatures (T_{min}), which are more sensitive to climate change than their mean values (IPCC, 2012). Therefore, given the limited coverage of purely in situ observations, it is necessary to determine whether reanalysis can fill the gaps in these databases (Donat et al., 2014). Xie et al. (2014) suggested that ERA Interim performs best in East Antarctica, after comparing these data with the other reanalysis for T_{mean}. Hence, we selected ERA Interim to evaluate extracted daily T_{min} and T_{max}, to determine whether ERA Interim could replicate temperature extremes in East Ant-

arctica during 2005–2008. This paper is structured as follows: We describe the data used and methods applied in the next section. The comparison of daily, annual, and seasonal T_{min} and T_{max} from observations and ERA Interim is presented in the following section, followed by a discussion of the results and the replication ability of ERA Interim. Major conclusions are summarized in the final section.

Data and Methodology

Observational Meteorological Data

China has carried out 32 expeditions in East Antarctica involving 11 traverses from Zhongshan Station on the coast to Dome Argus (Dome A) on the summit of the East Antarctica Ice Sheet. To improve incomplete meteorological records in this region, China deployed three automatic weather stations (AWSs), LGB69, EAGLE, and DOME A, along this route (Fig. 1). These stations are operated in collaboration with the Australian Antarctic Division. In addition to data from these three AWSs, we used data from Zhongshan Station for comparison with the ERA Interim reanalysis data set. Specifically, Zhongshan Station is on the East Antarctic coast, LGB69 is on the near-coastal escarpment of the ice sheet, EAGLE is within the interior region, and Dome A is on the summit of the East Antarctic Ice Sheet. These stations form a traverse along 77°E (Fig. 1). Xie et al., (2014) and (Xiao et al., 2008) provided details of the temperature sensors at these sites.

The surface air temperatures at the LGB69, EAGLE, and Dome A AWSs were recorded at hourly intervals at three nominal heights above the surface (1 m, 2 m, and 4 m). The daily minimum of the surface 2 m observation temperature was selected to compare with ERA Interim data in this study, because it reflects the surface energy balance and is closely related to snow temperature (Chen et al., 2010).

Assuming a log-linear temperature profile, all temperature observations were corrected for the effect of snow accumulation. Xie et al. (2014) and Ma et al. (2008) have given details for this correction. We also filtered the height-corrected data to eliminate outliers that are more than three standard deviations outside the average daily value for the study period covering 2005–2008. Over these four years of data, we have had only six outliers for daily air temperatures at Zhongshan Station, and none at the other three AWSs.

ERA Interim Dataset

The daily T_{min} and T_{max} at 2 m from ERA Interim are available from the ECMWF Data Server (http://apps.ecmwf.int/datasets/data/interim_full_daily/) as a T255 reduced Gaussian grid (Fig. 1). The ERA Interim reanalysis (1979 to present) was introduced to incorporate improvements to ERA-40, such as a refined data assimilation scheme and a refined numerical weather prediction model, a T255 spherical-harmonic representation for the basic dynamical fields, and an assimilation of Global Positioning System radio occultation measurements for atmospheric temperatures (Dee and Uppala, 2009; Dee et al., 2011; Poli et al., 2010; Uppala et al., 2005). All the 2 m T_{min} and T_{max} data used in this study were averaged into monthly, seasonal, and annual values. All four AWSs are located in different grids of ERA Interim reanalysis (Fig. 1).

Methodology

Corrections for the difference in elevation between the in situ measurement point and the grid cell average might make point measurements and reanalysis products (at different horizontal resolutions) more compatible. However, in this study the reanalysis of surface air temperature was directly compared with the observations without interpolation, for the following reasons: (1) Compared with other areas covered by glaciers or ice caps, such as mid-latitude mountains, Antarctica has very low topographic relief, especially in the Dome A area, which has a surface slope of less than 0.009% (Zhang et al., 2007). (2) Different interpolation methods may introduce new errors because of the assumptions in the correction (Wang and Zeng, 2012; Zhao et al., 2008). (3) Some new errors may also be introduced due to height differences between the different reanalysis grids. (4) The in situ stations lie in different grid points for each reanalysis. Hence, we focused on the basic evaluation of reanalysis, and

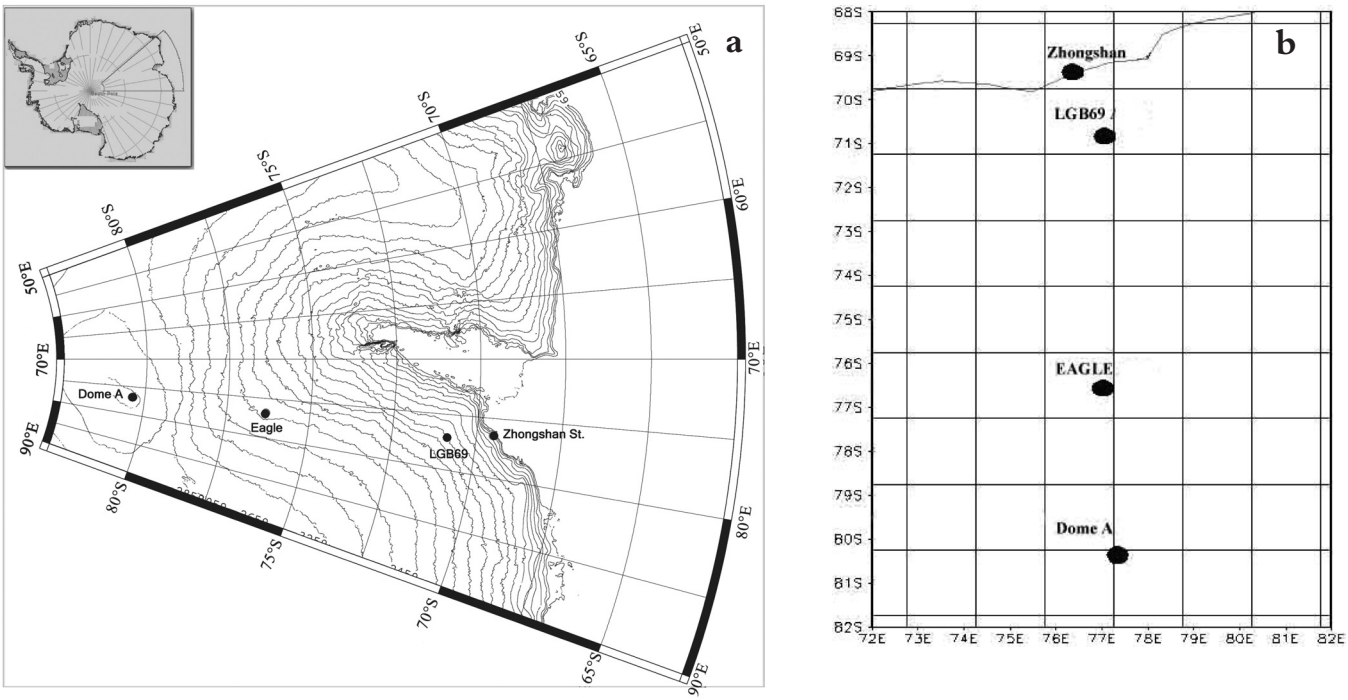

FIGURE 1. Locations of the Automatic Weather Stations along the traverse from Zhongshan Station to Dome A, and with superimposed ERA Interim reanalysis grids (T255 Gaussian grid, 1.5° × 1.5°).

the observed data were directly compared with those from the grid cell covering the site, with neither elevation correlation nor interpolation (Xie et al., 2014).

Surface daily T_{min} and T_{max} statistics for the reanalysis and observational data were examined to assess the daily, annual, and seasonal performance. In each case, root-mean-square error (RMSE), correlation coefficient (R), explained variance (square of the correlation coefficient, R^2), and bias were calculated for ERA Interim at each AWS site. Here, RMSE is defined as the square root of the mean-squared difference between the extracted reanalysis temperatures and the actual observations, effectively combining the errors of low correlation and high bias into one statistic (Bromwich and Fogt, 2004). R indicates whether the reanalysis and observation fields have similar patterns of variation, while R^2 indicates what percentage of variance the reanalysis can explain. Bias is the mean reanalysis value over a given period minus the mean observed value. The indices of the normalized RMSE, R, and the ratio of the variances are summarized in a Taylor diagram, which displays the three statistics on a two-dimensional plot based on the Law of Cosines (Taylor, 2001). A Taylor diagram provides a visual framework to evaluate ERA Interim T_{min} and T_{max} with respect to their corresponding field or observational values. An observation is represented by a point at unit distance from the origin along the abscissa. All other points, representing ERA Interim data are placed such that the ratio of the variances of ERA Interim data and observation is given by the radial distance from the origin. Errors are depicted by the pattern of points about the observed point. Thus, when the distance to the point representing the observation is short, there is good agreement between the reanalysis and the observation. For more details, refer to http://www.ncl.ucar.edu/. The plotted values are derived from monthly means of daily T_{max} and $T_{min.}$

The Cross-correlation function (CCF) is used here to analyze the time delay between ERA Interim and in situ observations, as a measure of similarity of two series in signal processing. For continuous functions f and g, the cross correlation is defined as:

$$(f \star g)(\tau) \stackrel{def}{=} \int_{-\infty}^{\infty} f^{\star}(t) g(t+\tau) dt, \qquad (1)$$

where f^* denotes the complex conjugate of f, and τ is the lag. Based on the CCF analysis, we have generated the Cross-correlation plots to describe clearly the performance of ERA Interim, according to the Cross-correlation coefficients (CCCs). When peaks (positive areas) are aligned, they make a large contribution to the integral. Similarly, when troughs (negative areas) align, they also make a positive contribution to the integral, because the product of two negative numbers is positive.

Results and Discussions

For our analysis, we used daily, monthly, seasonal, and annual values of 2 m daily T_{min} and T_{max} observations (Table 1) for the period from 2005 to 2008. These data show an expected decrease in temperature with increasing altitude and latitude. During the study period, observational extreme daily T_{min} was –45.7 °C, –47.1 °C, –67.7 °C, and –81.5 °C at Zhongshan Station, LGB69, EAGLE and Dome A, respectively. The corresponding T_{max} was 8.7 °C, –3.7 °C, –10.4 °C, and –18.4 °C, while the observational mean daily temperature range was 4.6 °C, 5.2 °C, 8.4 °C, and 9.7 °C for these four sites. T_{min} and T_{max} both decreased, and daily temperature range increased, with increasing altitude and latitude, as expected.

Daily and Annual Performance of ERA Interim T_{min} And T_{max}

Figure 2, part a, shows the daily T_{min} biases between the ERA Interim reanalysis and field observations at the four sites. Clearly, the ERA Interim data overestimated daily T_{min}, with a mean warm bias of 4.4 °C for all four stations. ERA Interim performed best at Zhongshan Station (Fig. 3, part a), where it had the lowest bias of 1.0 °C, explaining more than 92.7% of the variance (Table 2). However, on average, ERA Interim overestimated daily T_{min}, although it showed some underestimations at Zhongshan Station. The maximum daily negative bias was –4.9 °C on 26 September 2007, whereas the maximum positive bias was 18.0 °C on 30 July 2005, coinciding with a low temperature extreme event. ERA Interim consistently overestimated values at LGB69 and EAGLE, with only occasional underestimations (Fig. 3, part a). At these sites, the warm bias was as large as 5.7 °C and 6.9 °C, respectively. However, the explained variance was more than 88%. In terms of explained variance, ERA Interim performed worst at Dome A (87.5%), although the warm bias was small (4.1 °C) (Table 2), as ERA Interim alternately overestimated and underestimated daily T_{min}. ERA Interim had average RMSE of 2.4 °C, 2.6 °C, 3.0 °C and 4.3 °C at Zhongshan, LGB69, EAGLE, and Dome A, respectively (Table 2). This indicates that errors increased with increasing distance from the coast to the interior of the East Antarctic Ice Sheet. In situ surface meteorological observations are sparse in the East Antarctic interior, decreasing with increasing latitude and altitude. This causes likely errors to increase from the coast to the summit of the ice sheet. The warm bias in daily T_{min} shows that ERA Interim data underestimated the strength of daily temperature drop. In this study, reanalysis T_{min} val-

TABLE 1

Annual, seasonal,* and monthly observed T_{min} and T_{max} (°C) for Zhongshan Station, LGB69, EAGLE, and Dome A.

		Annual	Spring	Summer	Autumn	Winter	Jan	Feb	Mar	Apr	May	Jun	Jul	Aug	Sep	Oct	Nov	Dec
T_{min}	Zhongshan	–11.9	–13.7	–2.8	–13.1	–17.8	–1.7	–5.0	–9.3	–13.1	–16.7	–16.2	–18.2	–19.1	–18.7	–15.1	–7.1	–2.1
	LGB69	–28.8	–29.2	–21	–31.6	–34.9	–19.2	–24.4	–28.9	–32.3	–34.6	–34.0	–35.2	–36.0	–34.3	–31.1	–24.5	–19.3
	EAGLE	–45.7	–47.1	–33.3	–49.2	–52.1	–30.5	–40.0	–45.8	–49.8	–51.7	–50.8	–51.6	–54.1	–53.9	–50.2	–37.1	–29.5
	Dome A	–57	–58.2	–42.8	–61.3	–64.9	–40.2	–50.3	–58.5	–61.9	–63.5	–63.4	–64.7	–66.7	–66.7	–60.3	–47.4	–38.2
T_{max}	Zhongshan	–7.3	–8.5	1.4	–8.7	–13.1	2.7	–1.2	–5.5	–8.8	–11.6	–11.9	–13.3	–14.3	–13.5	–9.9	–1.9	2.4
	LGB69	–23.6	–24.2	–14.8	–26.3	–31	–13.3	–16.9	–22.5	–26.9	–30.5	–30.5	–31.3	–31.8	–30.2	–26.0	–19.0	–14.3
	EAGLE	–37.3	–36.3	–23.4	–42.3	–45.9	–20.9	–29.4	–37.7	–43.2	–45.9	–44.6	–45.4	–47.8	–45.8	–37.4	–25.8	–20.1
	Dome A	–47.4	–46.4	–32.8	–52.5	–56.9	–30.4	–39.2	–48.9	–53.5	–54.9	–55.2	–56.7	–58.8	–56.2	–47.2	–35.8	–29.1

*Austral seasons are spring (September to November), summer (December to February), autumn (March to May), and winter (June to August).

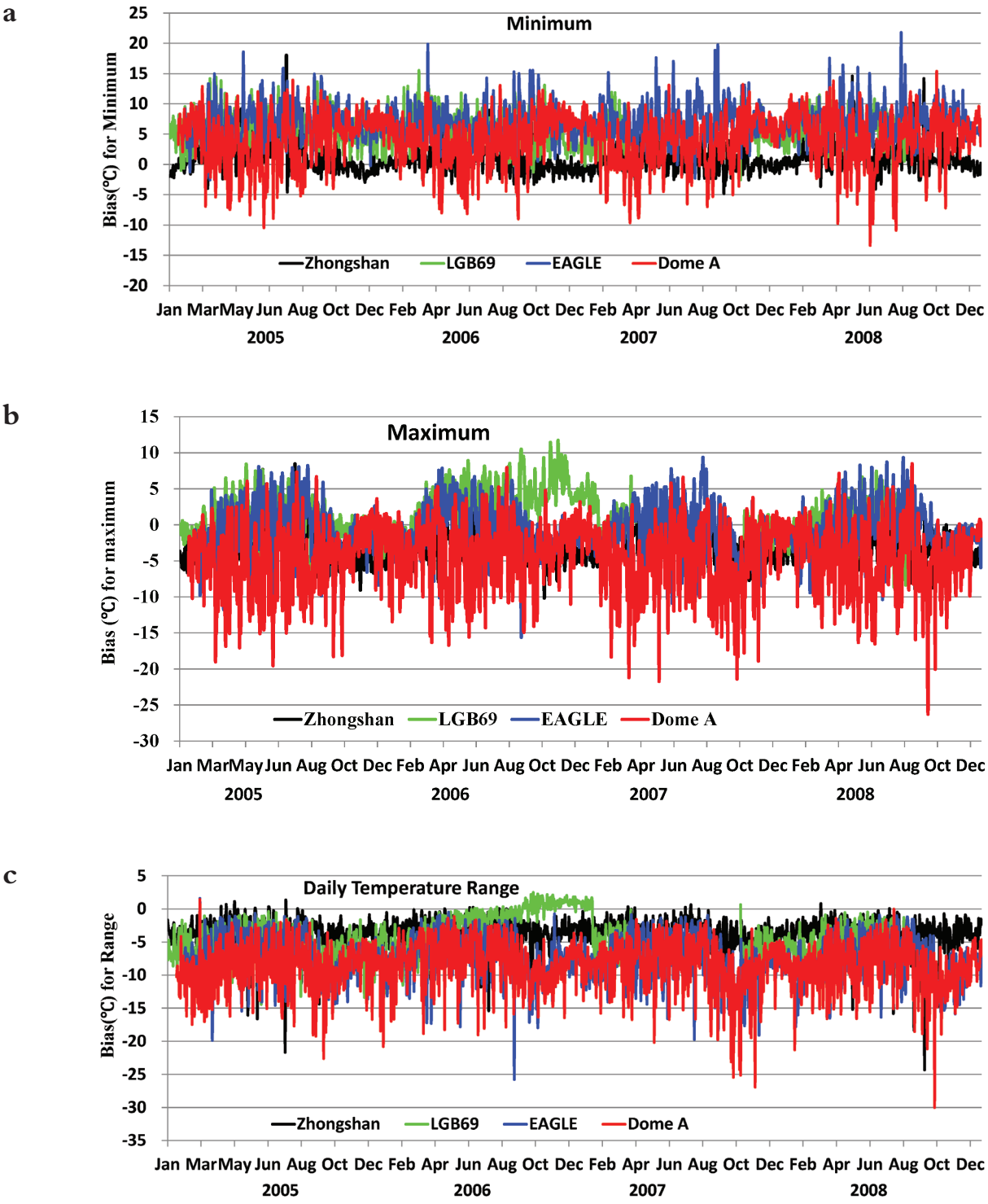

FIGURE 2. Daily biases (°C) between ERA Interim and field observations over four years (2005–2008) at Zhongshan Station (black), LGB69 (green), EAGLE (blue) and Dome A (red) for (a) T_{min}, (b) T_{max}, and (c) daily temperature range.

ues are compared directly with field observations, without interpolation. However, Zhongshan Station, LGB69, and EAGLE are all located south of and higher in elevation than the center points of their respective ERA Interim grids (Fig. 1), which may explain in part the warm biases in the reanalysis values for T_{min}. However, Dome A is located north of and lower in elevation than its grid center

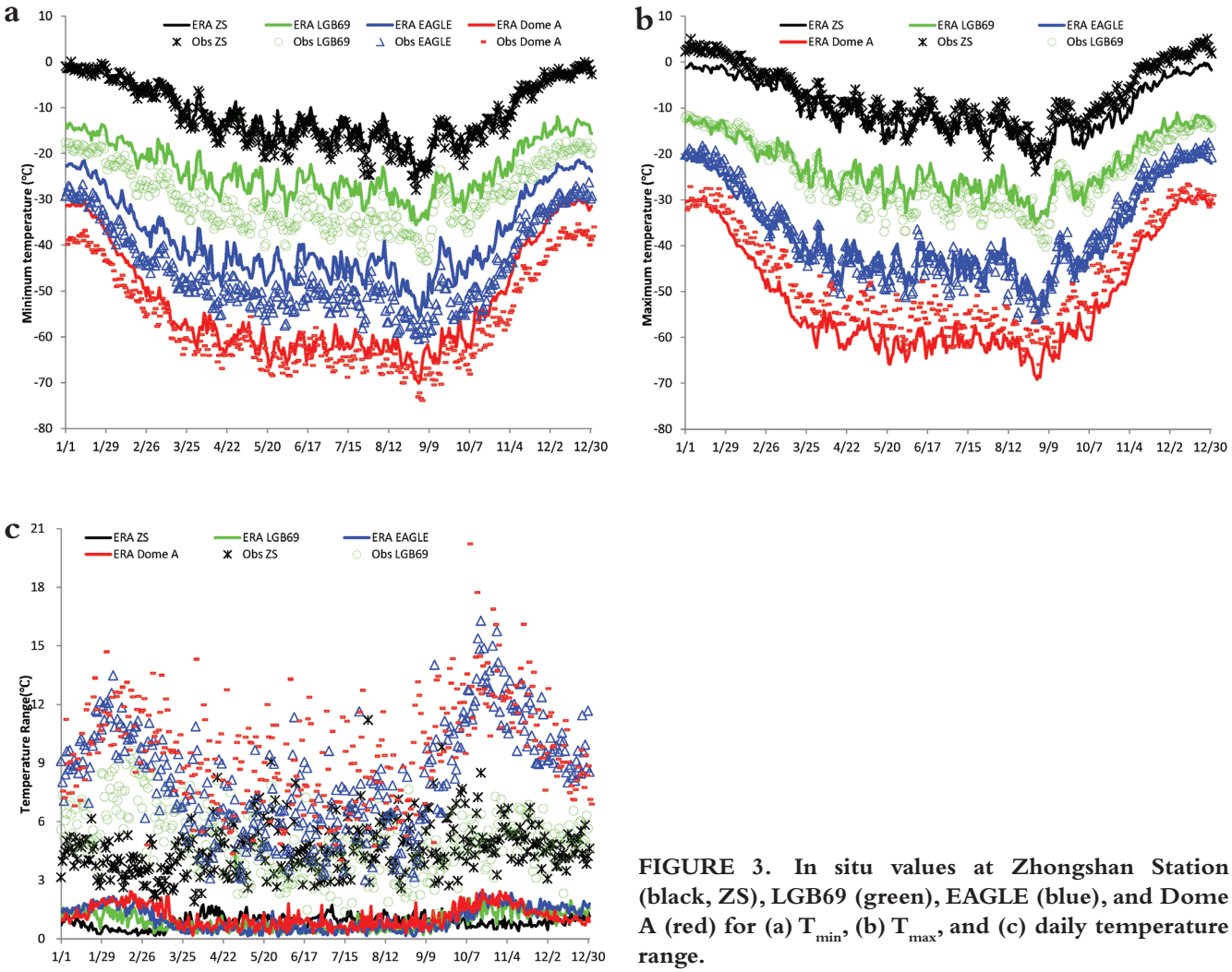

FIGURE 3. In situ values at Zhongshan Station (black, ZS), LGB69 (green), EAGLE (blue), and Dome A (red) for (a) T_{min}, (b) T_{max}, and (c) daily temperature range.

point (Fig. 1). The consistent warm bias of T_{min} data indicates that location within ERA Interim grids may affect values, but it is neither the only factor nor an important factor.

Typically, daily T_{max} was underestimated by ERA Interim (Figs. 2, part b, and 3, part b), with cool biases of 2.8 °C, 0.5 °C, and 4.4 °C at Zhongshan, EAGLE, and Dome A, respectively. Meanwhile, ERA Interim T_{max} showed a mean warm bias of 1.4 °C at LGB69. On average, ERA Interim alternately overestimated and underestimated the daily T_{max}, giving RMSEs of 3.1 °C and 3.4 °C at LGB69 and EAGLE. Similar to T_{min}, T_{max} was best replicated at Zhongshan Station, with a RMSE of 2.2 °C and an explained variance of 92.6% (Table 2). ERA Interim consistently underestimated T_{max}, with only occasional overestimation in winter and autumn at Zhongshan Station. ERA Interim performed worst at Dome A, with a RMSE of 4.9 °C and an explained variance of 84.1% (Table 2). Hence, the cool biases in daily T_{max} indicate that ERA Interim underestimated the strength of the daily temperature rise. Dome A was located north of and lower in elevation than the grid center point, whereas LGB69 was located south of and higher in elevation than the grid center point for ERA Interim data (Fig. 1), which may explain the cool bias at Dome A and the warm bias at LGB69 in the reanalysis T_{max}. However, Zhongshan Station and EAGLE were both located south of and higher in elevation than their grid center points (Fig. 1), suggesting again that interpolation is not an important factor affecting T_{max} in our comparison.

Given the warm bias of daily T_{min} and the cool bias of daily T_{max}, ERA Interim clearly underestimated the daily temperature range, usually with a negative bias, but occasionally with a positive one (Figs. 2, part c, and 3, part c). ERA Interim

TABLE 2

Bias (°C) and root mean square error (RMSE; °C) between ERA Interim and field observations, and the explained variance (%) of ERA Interim results at the four weather stations.

		Daily Minimum			Daily Maximum		
		Bias (°C)	RMSE (°C)	Explained variance (%)	Bias (°C)	RMSE (°C)	Explained variance (%)
Annual	Zhongshan	1.0	2.4	92.7	–2.8	2.2	92.6
	LGB69	5.7	2.6	88.3	1.4	3.1	86.0
	EAGLE	6.9	3.0	91.7	–0.5	3.4	92.4
	Dome A	4.1	4.3	87.5	–4.4	4.9	84.1
	Average	4.4	3.1	90.1	–1.6	3.4	88.8
Spring	Zhongshan	0.5	2.2	91.1	–3.9	1.9	92.1
	LGB69	5.7	2.9	80.5	2.0	3.4	76.5
	EAGLE	7.5	3.0	90.3	–1.9	2.8	93.3
	Dome A	5.1	3.9	86.7	–5.2	4.8	80.8
	Average	4.7	3.0	87.1	–2.2	3.2	85.7
Summer	Zhongshan	–0.1	1.1	87.4	–3.6	1.4	80.9
	LGB69	4.8	2.3	69.4	–0.2	2.7	50.7
	EAGLE	6.4	1.9	90.0	–1.9	1.6	90.9
	Dome A	6.4	2.6	84.3	–2.2	3.3	72.2
	Average	4.4	2.0	82.8	–2.0	2.3	73.7
Autumn	Zhongshan	1.5	2.2	87.9	–2.0	1.8	88.2
	LGB69	6.4	2.6	80.4	1.7	2.7	82.3
	EAGLE	6.8	3.2	75.9	0.5	3.5	82.0
	Dome A	2.4	4.5	42.5	–5.6	5.2	40.0
	Average	4.3	3.1	71.7	–1.3	3.3	73.2
Winter	Zhongshan	2.0	2.8	83.8	–1.7	2.4	87.3
	LGB69	6.0	2.3	82.8	2.6	3.2	70.3
	EAGLE	6.7	3.4	77.0	1.0	4.1	74.3
	Dome A	2.7	4.5	44.5	–4.6	5.4	33.9
	Average	4.3	3.2	72.0	–0.7	3.8	66.4

had mean biases of –3.8 °C, –4.3 °C, –7.4 °C, and –8.5 °C for daily temperature range at Zhongshan, LGB69, EAGLE, and Dome A, respectively. This suggests that underestimation of daily temperature range increased with increasing altitude, latitude, and distance from the coast across the East Antarctic Ice Sheet. This is consistent with in situ surface meteorological observations that decrease with increasing latitude and altitude (Fogt et al., 2016).

Although ERA Interim explains more than 84% of daily and annual variance, there are always inevitable errors and RMSEs between reanalysis and observations. This can reflect three mismatch types: Scale/spatial mismatch occurs when the observational data refer to temperatures measured at specific points, while ERA Interim data provide an average value over a grid cell. Temporal mismatch occurs when daily T_{min} and T_{max} are obtained from hourly observation values, while ERA

Interim data are often generated from different intervals. Topography mismatch occurs when topography in ERA Interim is different from the real landscape. Furthermore, the paucity of data toward the interior can also explicate the regional difference of performance of ERA Interim daily T_{min} and T_{max} and daily temperature range. The following two reasons are most significant: (1) The stations over the Antarctic continent are confined mainly to coastal margins, and huge interior areas are devoid of long-term, in situ tropospheric temperature observations (Fogt et al., 2016). (2) There are no observations poleward of 82.5° from the polar orbiting satellites (Johanson and Fu, 2007), hence ERA Interim reanalysis is devoid of one of the most important data sets that could be assimilated (Dee et al., 2011).

Assessment of the Monthly and Seasonal Performance of ERA Interim T_{min} And T_{max}

Figure 4 shows the explained variance (%) and *RMSE* (°C) for ERA Interim reanalysis data compared with monthly observations for T_{min} and T_{max} in the austral spring (September–November, SON), summer (December–February, DJF), autumn (March–May, MAM), and winter (June–August, JJA) seasons. Monthly ERA Interim T_{min} performed similarly to T_{max} in terms of explained variance. At Zhongshan Station and EAGLE, monthly ERA Interim accounted for more than 60% variance, with no obvious seasonal variability. At Dome A, ERA Interim displayed marked monthly variability, with the lowest variance scores in April (26.7% for T_{min} and 20.3% for T_{max}), and highest variance scores in November (75.7% for T_{min} and 56.7% for T_{max}). At LGB69, ERA Interim exhibited the largest range in variance, with lowest variance scores in January (39.1% for T_{min} and 12.7% for T_{max}) and higher ones in autumn and winter (more than 60% for T_{min} and T_{max}). Thus, reciprocal seasonal trends are observed at LGB69 and Dome A.

In contrast, monthly RMSEs of ERA Interim for T_{min} and T_{max} (Fig. 4) show less monthly variability, especially at LGB69. In general, the monthly RMSE for ERA Interim T_{max} is large at Dome A, but smaller at the other three sites. The performance of T_{max} at the three sites is similar to that of T_{mean} (Xie et al., 2014).

Figure 5 presents Taylor diagrams summarizing the performance of ERA Interim reanalysis for the austral seasons of spring, summer, autumn, and winter. The scatter of points varies with each season. In general, points are more clustered in spring and more scattered in summer. In autumn and winter, points are clustered, except for some at Dome A (stars). Figure 5 confirms that ERA Interim corresponds best with observations in spring, having high correlation coefficients and low RMSEs, and explaining more than 85% of the variance (Table 2), especially at Zhongshan Station and EAGLE. ERA Interim performs worst in autumn and winter, especially at Dome A, where less than 34% of the variance is explained (Fig. 5, Table 2). The seasonal differences in performance of ERA Interim T_{min} and T_{max} are very similar to that of T_{mean} (Xie et al., 2014), and it may in fact be worse for T_{mean} because of temperature extremes.

Several factors contribute to the seasonal performance, which was worse in autumn/winter than in summer. During winter, in the absence of solar radiation, the most prominent element of the climate of East Antarctica is the near-surface temperature inversion of up to 30 K (Allison, 1998; Connolley, 1996), and the phenomena is persistent (Allison, 1998). In summer, the surface is in near-radiative balance, so that the horizontal and vertical potential temperature gradients are strongly reduced over the ice sheet and the coastal seas. Analysis of the heat budget elucidates the possible impact of inaccuracies of parameterizations on the model climate (Connolley, 1996;Van de Berg et al., 2007). In winter, the atmosphere is much colder and more stable compared to summer. As a result of the semiannual oscillation (SAO), the surface pressure in middle and high latitudes shows a clear half-yearly wave. In response to the variation in the meridional pressure gradient, the zonal westerlies show equinoctial maxima, which are 20–30% stronger than those in summer and winter (Van Den Broeke, 1998). In the seasons of SAO transition, the temperature field tends to be more complex, and is more difficult to simulate. The ECMWF parameterizations of clouds, longwave radiation, and turbulent mixing still have flaws in the cold and stable atmosphere

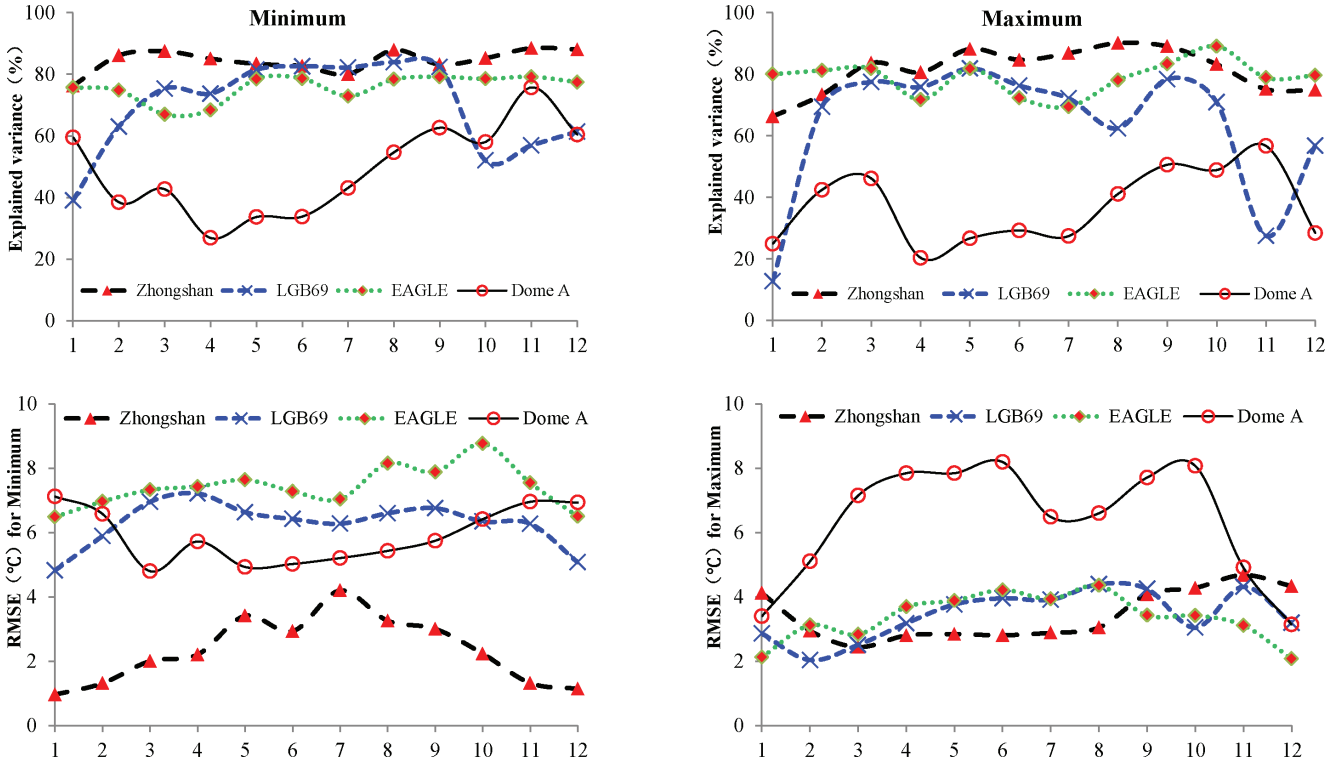

FIGURE 4. (top, a and b) Monthly variance and (bottom, c and d) root mean square error (RMSE) explained by ERA Interim at Zhongshan (black dashed line with red triangle), LGB69 (blue dashed line with blue cross), EAGLE (green dotted line with red rhomboid) and Dome A (black solid line with open red circle) for (left, a and c) T_{min} and (right, b and d) T_{max}.

over the East Antarctic Ice Sheet (Bromwich et al., 2012;Van de Berg et al., 2007). From spring to autumn, when incoming shortwave radiation dominates over longwave cooling, T_{max} increases with decreasing opaque cloud cover, while T_{min} is almost independent of cloud cover. During the winter period, both T_{min} and T_{max} fall with decreasing cloud cover, as longwave cooling dominates over the net shortwave flux, which is reduced by the high solar zenith angle and surface reflection by snow (Betts et al., 2013).

Special Cases of the Temperature Extremes from ERA Interim

Based on the extreme temperature indices commonly used (IPCC, 2012;You et al., 2010) and the weather/climate in Antarctica, we define cooling or warming as weather extremes, if temperatures at all four stations have abrupt drops/rises of more than 10 °C within 24 hours, and last for more than 3 days. From 2005 to 2008, 8 cooling and 11 warming extremes occurred (data not shown). Here we select one cooling and one warming extreme to evaluate ERA Interim reanalysis of these events.

The selected cooling weather extreme happened from 25 to 31 July 2005. During this extreme, field temperatures dropped by 28.6 °C, 14.9 °C, 24.3 °C, and 23.8 °C at Zhongshan Station, LGB69, EAGLE, and Dome A, respectively. The temperatures extracted from the ERA Interim fell by 16.8 °C, 20.2 °C, 16.8 °C, and 17.4 °C at these four stations. Figure 6 shows the spatial distribution of temperatures extracted from the ERA Interim at 500 hPa, with the wind field along the 77°E meridional profile. Compared with earlier data from 17 to 24 July (Fig. 6, part a), the spatial distribution of the ERA Interim temperature during the extreme weather (Fig. 6, part b) shows that the low temperature center strengthened and moved eastward to the region of the research AWSs in East Antarctica, and then expanded and lessened from 1 to 7 August (Fig. 6, part c). The wind field along the vertical profile of the 77°E meridian (Fig. 6, parts d, e, and f) also changed, especially

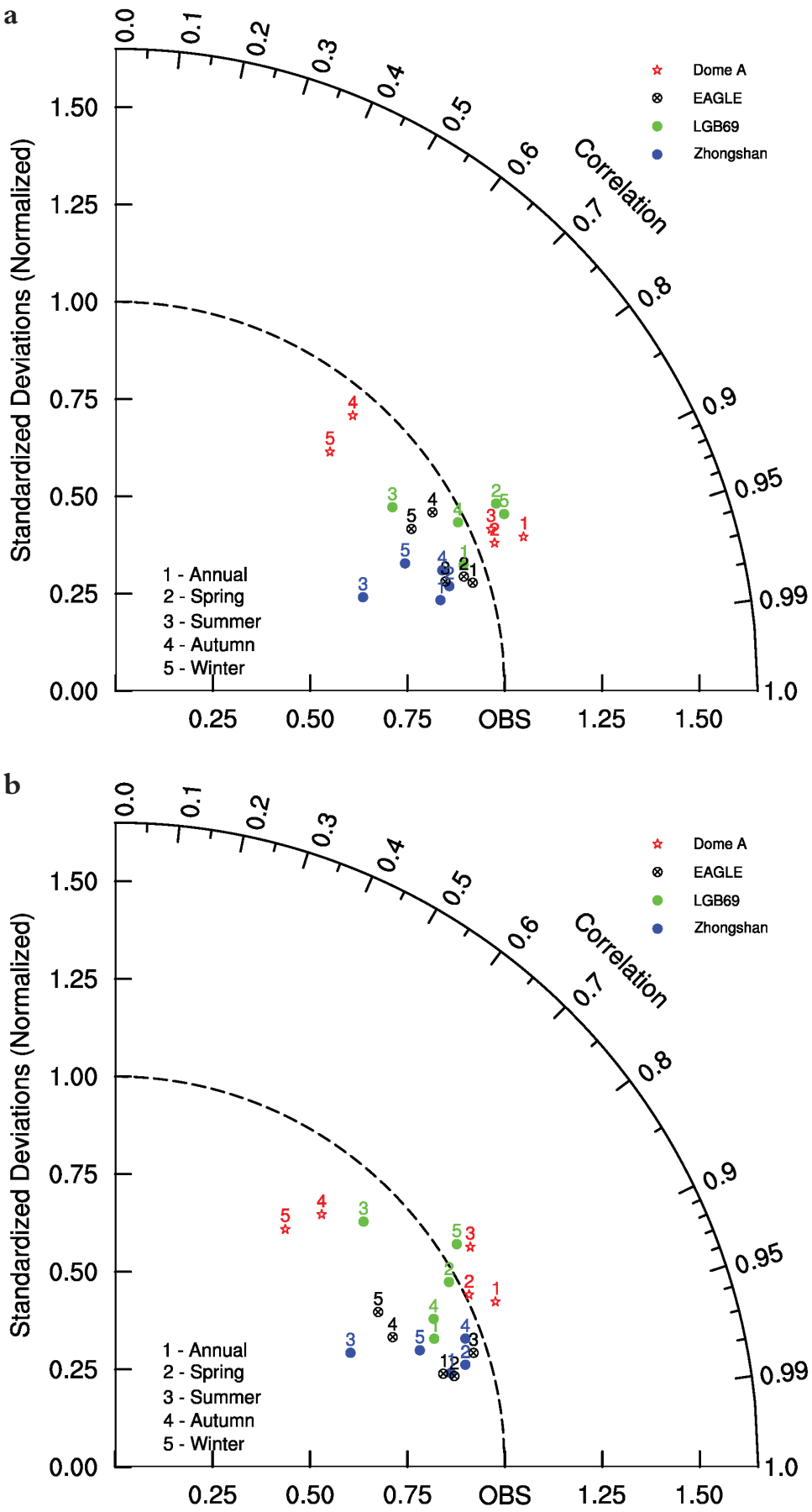

FIGURE 5. Taylor diagrams showing correlation coefficients, standard deviation, and root-mean-square error (RMSE) of mean (a) T_{min} and (b) T_{max} extracted from ERA Interim. The radial coordinate gives the magnitude of total standard deviation, normalized by the observed value, while the angular coordinate gives the correlation with the observation. It follows that the distance between the observed point and ERA Interim point is proportional to the RMSE. Numbers 1, 2, 3, 4, and 5 indicate annual, spring, summer, autumn, and winter T_{min} (a) and T_{max} (b), compared with their corresponding observations at Zhongshan Station (closed blue circle), LGB69 (closed green circle), EAGLE (black circle with cross), and Dome A (red star).

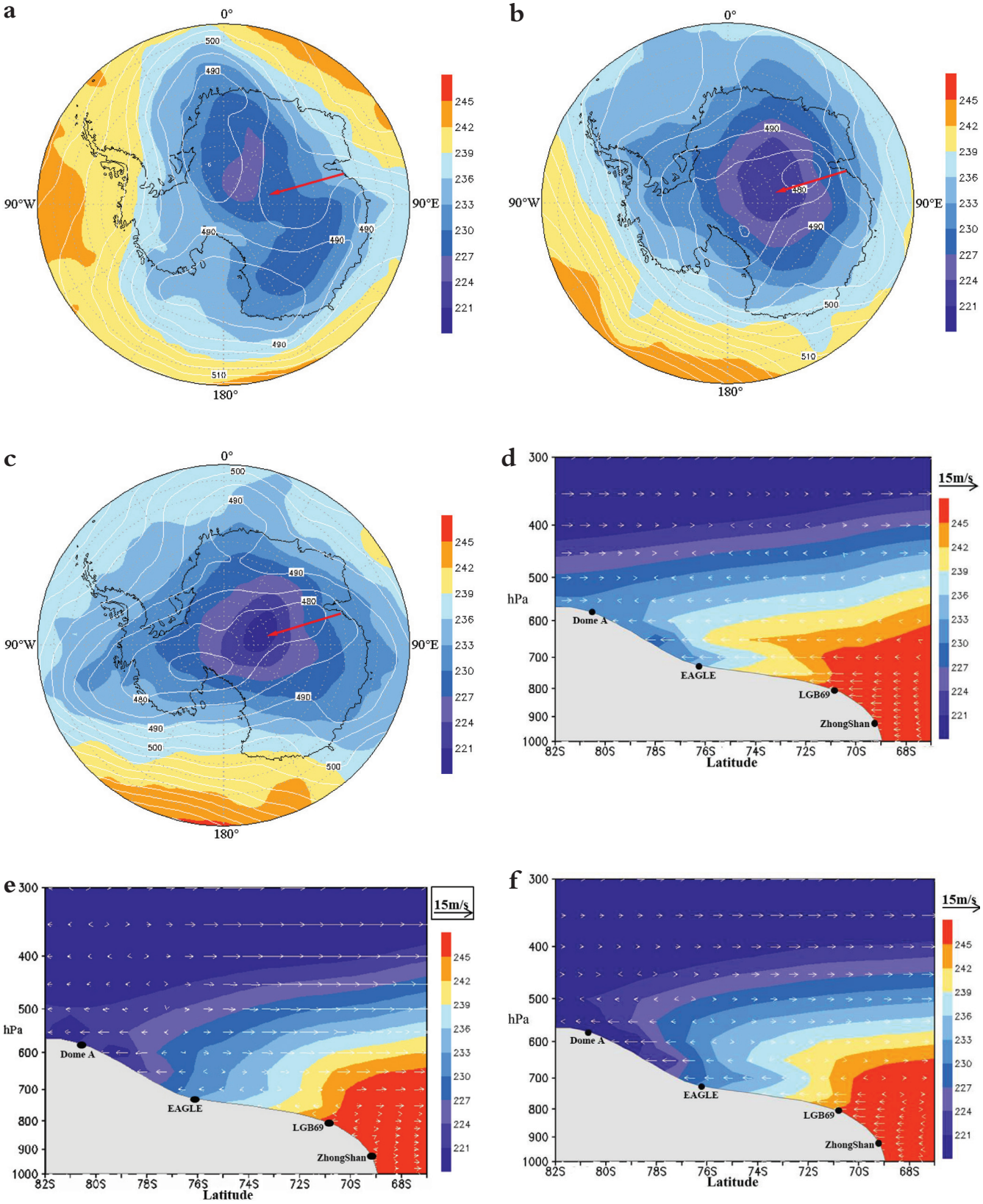

FIGURE 6. (a, b, and c) Spatial distributions of mean temperature at 500hPa, with red arrows representing the region from Zhongshan Station to Dome A, as well as (d, e, and f) wind profiles along the 77°E meridional profile, where black dots show stations during the temperature fall in July 2005, with data covering the period from 17 July to 7 August 2005. NB: a and d show data for 17 to 24 July (before the extreme); b and e show data for 25 to 31 July (during the extreme); and c and f show data for 1 to 7 August (after the extreme).

at lower levels near Zhongshan Station. During the extreme weather (Fig. 6, part e), wind blew from the interior to the coast. The shift in the wind field from ERA Interim reanalysis is consistent with such observations (not shown).

A warming weather extreme occurred from 9 to 11 June 2007. During this extreme, field temperatures increased by 10.6 °C, 28.6 °C, and 22.7 °C at Zhongshan, EAGLE, and Dome A, respectively. There were no observational data at LGB69 for this period. Temperatures from the ERA Interim were elevated by 9.2 °C, 21.7 °C, and 16.9 °C at Zhongshan Station, EAGLE, and Dome A, respectively. Changes in temperature and wind field during this warm extreme are shown in Figure 7.

Thus, the ERA Interim replicates both these cool and warm weather extremes in East Antarctica, although sudden jumps in the temperature record are difficult to find (Johanson and Fu, 2007). However, as an assimilated product including the adaptive estimation of data numbers from many sources (Uppala et al., 2005), ERA Interim inevitably underestimates the strength of cooling or warming. In addition to the reasons for the underestimation from three mismatch types (scale/spatial, temporal, topographical) mentioned in the previous section, the uncertainties from clouds play an important role. Through their shortwave and longwave radiative properties, clouds influence the temperature of atmosphere, and the microphysical properties of cloud particles can have a major impact on the ice sheet's radiation budget (Bromwich et al., 2012; Lachlan-Cope, 2010; Van Wessem et al., 2014). It is therefore important that they are correctly represented in climate models.

Specific Weather Events of ERA Interim T_{min} And T_{max}

Figure 8 displays cross correlations for all the daily T_{min} and T_{max} from ERA Interim and the field data for all four AWSs. Cross-correlation functional (CCF) analysis confirms that cool weather events (Moore, 2004; Moore and Semple, 2006) extracted from the ERA Interim appeared on the same days as observations (Fig. 8, top row). Cross-correlation coefficients (CCCs) are 0.618 (N = 1461, P < 0.001) at Zhongshan, 0.424 (N = 1131, P < 0.001) at LGB69, 0.502 (N = 1434, P < 0.001) at EAGLE, and 0.287 (N = 1445, P < 0.001) at Dome A, respectively. The cool weather events in the reanalysis data sometimes occurred two days ahead of observations at Zhongshan Station with a CCC of –0.275 (N = 1461, P < 0.001), or one day ahead at LGB69, EAGLE, and Dome A, with CCCs of –0.316 (N = 1131, P < 0.001), –0.425 (N = 1434, P < 0.001), and –0.237 (N = 1445, P < 0.001), respectively. In general, the explained variance of the ERA Interim for cool weather events decreases from the coast to the interior of the East Antarctic Ice Sheet.

Similar to daily T_{min}, warm weather events reflected in the ERA Interim T_{max} (Fig. 8, bottom row) occurred on the same days as the observations, with a CCC of 0.617 (N = 1461, P < 0.001) at Zhongshan Station, 0.442 (N = 1131, P < 0.001) at LGB69, and 0.384 (N = 1434, P < 0.001) at EAGLE, respectively. Warming weather events from the ERA Interim appeared one day ahead of observations, with a CCC of –0.219 (N = 1461, P < 0.001) at Zhongshan and –0.293 (N = 1131, P < 0.001) at LGB69, respectively. However, for EAGLE observations, the CCCs for T_{max} are –0.346, 0.343, 0.384, and –0.329 for events occurring with a two day lag, one day lag, no lag, and 1 day ahead, respectively. These CCCs show that the ERA Interim can explain similar variance over four days. At Dome A, the explained variance of the ERA Interim was smaller than for other stations, although the CCCs over the five days exceeded the confidence limits.

Conclusively, the weather events in East Antarctica extracted from the ERA Interim data set for retrospective periods occurred mainly on the same day as indicated by field observations. This is very practical from the standpoint of improving the safety of researchers and travelers in East Antarctica for both scientific and recreational purposes, using various weather products. In the meantime, the ability of the ERA Interim to predict/forecast weather events will diminish with increasing distance from the coast, in a manner similar to the daily to annual performances of the ERA Interim for temperature data presented in this study.

Conclusions and Discussion

Comparison of daily 2 m T_{min} and T_{max} from the ERA Interim reanalysis against in situ observations from 2005 to 2008 at Zhongshan Station, LGB69,

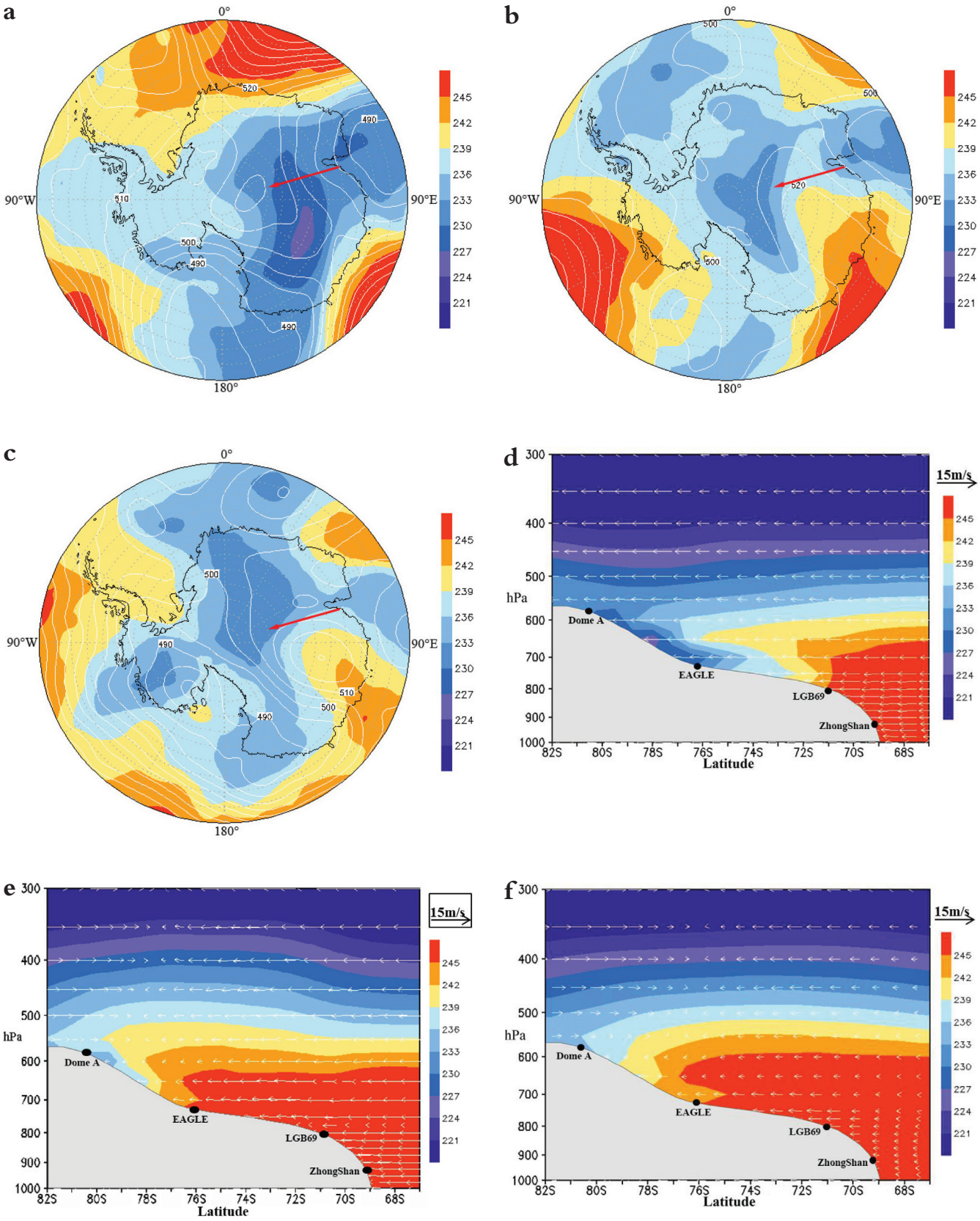

FIGURE 7. As for Figure 6 but for an extreme rise in temperature from 6 to 14 June 2007. NB: a and d show data for 6 to 8 June (before the extreme); b and e show data for 9 to 11 June (during the extreme); and c and f show data for 12 to 14 June (after the extreme).

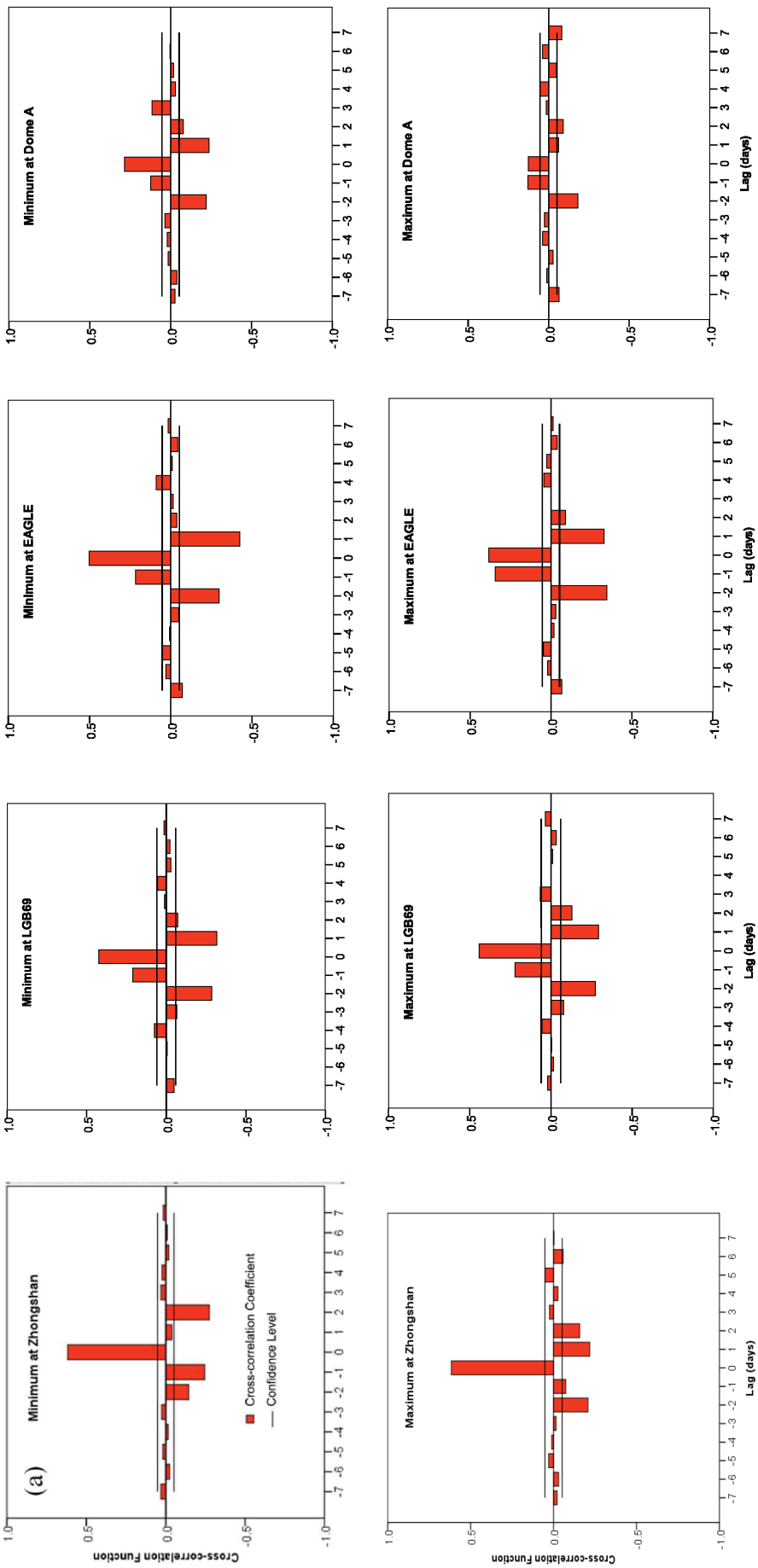

FIGURE 8. Cross-correlation plots between field observations and ERA Interim reanalysis for daily minimum (top plots) and maximum (bottom plots) temperature (°C) at the four weather stations in East Antarctica from 2005 to 2008. The rectangles indicate the cross-correlation coefficient, while the lines represent confidence limits.

EAGLE, and Dome A in East Antarctica demonstrates that:

(i) The ERA Interim captured daily and annual T_{min} and T_{max} variations, with a variance explained of more than 84%. Annual average RMSEs of 2.4 °C, 2.6 °C, 3.0 °C, and 4.3 °C for daily T_{min}, and 2.2 °C, 3.1 °C, 3.4 °C, and 4.9 °C for daily T_{max} were calculated based on observational data from Zhongshan Station, LGB69, Eagle, and Dome A, respectively. This suggests that errors in the ERA Interim increased from the coast to the interior of the East Antarctic Ice Sheet.

(ii) Little seasonal variability was observed in the performance of the ERA Interim for T_{min} and T_{max} except at the summit site (Dome A), where performance was best in the austral spring and worst in winter and autumn.

(iii) The spatial distribution of temperatures and wind fields from the ERA Interim replicated the evolution of temperature extremes, as they developed, persisted, and disappeared in this region.

(iv) Weather events extracted from the ERA Interim occurred mainly on the same day as observations, having a high cross-correlation coefficient ($R \geqq 0.287$, $N \geqq 1131$, $P < 0.001$). The performance of the ERA Interim showed clear regional trends, worsening from the coast to the interior of the East Antarctica Ice Sheet.

Despite its regional limitations in T_{min} and T_{max} in East Antarctica, we show that the ERA Interim is still a powerful tool for weather and climate studies in this region.

Clouds in extreme southern latitudes, however, are still poorly understood, because of the following reasons: (1) There are relatively few measurements of clouds in the Antarctic, because of Antarctica's remoteness and challenging environment (Bromwich et al., 2012). (2) Model cloud parameterizations are often based empirically on measurements made in the Tropics and middle latitudes, so that their applicability for Antarctic clouds is questionable (Lachlan-Cope, 2010). (3) The ERA Interim is constrained by a wide variety of atmospheric observations such as radiosoundings and satellite radiances. Nonetheless, clouds are produced by the reanalysis model short-term forecasts and are thus strongly influenced by the model physics (Dee et al., 2011). (4) From the Antarctic perspective, observations suggest that polar clouds are highly sensitive to the number concentration of ice nuclei (IN). Fewer IN in clouds are present at low temperatures, and realistic simulations are possible for Antarctica (Guo et al., 2003). However, not surprisingly, early attention has focused more on the Arctic (Morrison et al., 2008), and little on the Antarctic. (5) The cloud impact on radiation may not be well simulated by the Polar WRF (Wilson et al., 2012). The ensemble average generally overestimates the cloud amount over the Antarctic continent by 10%–15%, and the excess of clouds over Antarctica may be, in part, due to the coarse resolution of the atmospheric models, resulting in a smoothing of the ice sheet's topography and an excessive influx of moisture inland (Bromwich et al., 2012). (6) Verification of modeled prognostic clouds versus observations can be problematic. There are difficulties associated with obtaining objective cloud observations, which are frequently reported in fractions or octas. In addition, many modern cloud prediction schemes predict the mass of water substance but do not directly produce a cloud fraction that can be compared to observations (Bromwich et al., 2012). (7) To our knowledge, no studies have attempted to parameterize Antarctic clear-sky precipitation in this way, and only limited efforts have been attempted in the Arctic (Bromwich et al., 2012; Girard and Blanchet, 2001).

To acquire a thorough understanding of temperature extremes and weather, more in situ observations and model simulations are required in the vast inland regions of Antarctica. Furthermore, improvement in observation and computational technologies as well as analytical methods will help refine small-scale characteristics and processes of extreme events, enhancing our overall understanding and modeling of extreme events.

Acknowledgments

This research was funded by the National Natural Science Foundation of China (Grant nos. 41476164, 41671073, 41421061, 41425003, 41671063, and 41401079). Our sincere appreciation goes to Prof. Longhua Lu for providing the meteorological data from Zhongshan, to Prof. Tuo Chen for his insightful comments, and to Profs. Xianhong Meng and Qinglong You for helping to make the Taylor diagrams. The authors would like to acknowledge the

Chinese Arctic and Antarctic Administration, the National Oceanic and Atmospheric Administration (NOAA), the European Centre for Medium-Range Weather Forecasts (ECMWF), and the Japan Meteorological Agency for their operational reanalysis data sets.

References Cited

Allison, I., 1998: Surface climate of interior of the Lambert Glacier basin, Antarctica, from automatic weather station data. *Annals of Glaciology*, 27: 515–520.

Betts, A. K., Desjardins, R., and Worth, D., 2013: Cloud radiative forcing of the diurnal cycle climate of the Canadian Prairies. *Journal of Geophysical Research: Atmospheres*, 118(16): 8935–8953.

Boccara, G., Hertzog, A., Basdevant, C., and Vial, F., 2008: Accuracy of NCEP/NCAR reanalyses and ECMWF analyses in the lower stratosphere over Antarctica in 2005. *Journal of Geophysical Research*, 113(D20115): doi http://dx.doi.org/10.1029/2008JD010116.

Bromwich, D. H., and Fogt, R. L., 2004: Strong trends in the skill of the ERA-40 and NCEP–NCAR reanalyses in the high and midlatitudes of the southern hemisphere, 1958–2001. *Journal of Climate*, 17: 4603–4619.

Bromwich, D. H., Fogt, R. L., Hodges, K. I., and Walsh, J. E., 2007: A tropospheric assessment of the ERA-40, NCEP, and JRA-25 global reanalyses in the polar regions. *Journal of Geophysical Research*, 112(D10111): doi http://dx.doi.org/10.1029/2006JD007859.

Bromwich, D. H., Nicolas, J. P., Hines, K. M., Kay, J. E., Key, E. L., Lazzara, M. A., Lubin, D., McFarquhar, G. M., Gorodetskaya, I.V., Grosvenor, D. P., Lachlan-Cope, T., and van Lipzig, N. P. M., 2012: Tropospheric clouds in Antarctica. *Reviews of Geophysics*, 50(1): RG1004, doi http://dx.doi.org/10.1029/2011RG000363.

Cape, M. R., Vernet, M., Skvarca, P., Marinsek, S., Scambos, T., and Domack, E., 2015: Foehn winds link climate-driven warming to ice shelf evolution in Antarctica. *Journal of Geophysical Research–Atmospheres*, 120(21): 11037–11057.

Chen, B., Zhang, R., Sun, S., Bian, L., Xiao, C., and Zhang, T., 2010: A one-dimensional heat transfer model of the Antarctic Ice Sheet and modeling of snow temperatures at Dome A, the summit of Antarctic Plateau. *Science China Earth Sciences*, 53(5): 763–772.

Compo, G. P., Whitaker, J. S., Sardeshmukh, P. D., Matsui, N., Allan, R. J., Yin, X., Gleason, B. E., Vose, R. S., Rutledge, G., Bessemoulin, P., Brönnimann, S., Brunet, M., Crouthamel, R. I., Grant, A. N., Groisman, P.Y., Jones, P. D., Kruk, M. C., Kruger, A. C., Marshall, G. J., Maugeri, M., Mok, H.Y., Nordli, Ø., Ross, T. F., Trigo, R. M., Wang, X. L., Woodruff, S. D. and Worley, S. J., 2011: The Twentieth Century Reanalysis Project. *Quarterly Journal of the Royal Meteorological Society*, 137(654): 1–28.

Connolley, W. M., 1996: The Antarctic temperature inversion. *International Journal of Climatology*, 16: 1333–1342.

Cornes, R. C. and Jones, P. D., 2013: How well does the ERA-Interim reanalysis replicate trends in extremes of surface temperature across Europe? *Journal of Geophysical Research: Atmospheres*, 118(18): 10262-10276.

Dee, D. P., and Uppala, S., 2009: Variational bias correction of satellite radiance data in the ERA-Interim reanalysis. *Quarterly Journal of the Royal Meteorological Society*, 135(644): 1830–1841.

Dee, D. P., Uppala, S. M., Simmons, A. J., Berrisford, P., Poli, P., Kobayashi, S., Andrae, U., Balmaseda, M. A., Balsamo, G., Bauer, P., Bechtold, P., Beljaars, A. C. M., van de Berg, L., Bidlot, J., Bormann, N., Delsol, C., Dragani, R., Fuentes, M., Geer, A. J., Haimberger, L., Healy, S. B., Hersbach, H., Hólm, E.V., Isaksen, L., Kållberg, P., Köhler, M., Matricardi, M., McNally, A. P., Monge-Sanz, B. M., Morcrette, J. J., Park, B. K., Peubey, C., de Rosnay, P., Tavolato, C., Thépaut, J. N., and Vitart, F., 2011: The ERA-Interim reanalysis: configuration and performance of the data assimilation system. *Quarterly Journal of the Royal Meteorological Society*, 137(656): 553–597.

Donat, M. G., Sillmann, J., Wild, S., Alexander, L. V., Lippmann, T. and Zwiers, F. W., 2014: Consistency of temperature and precipitation extremes across various global gridded in situ and reanalysis datasets. *Journal of Climate*, 27(13): 5019–5035.

Fogt, R. L., Goergens, C. A., Jones, M. E., Witte, G. A., Lee, M. Y., and Jones, J. M., 2016: Antarctic station-based seasonal pressure reconstructions since 1905, part 1: reconstruction evaluation. *Journal of Geophysical Research–Atmospheres*, 121: 2814–2835.

Genthon, C., Town, M. S., Six, D., Favier, V., Argentini, S., and Pellegrini, A., 2010: Meteorological atmospheric boundary layer measurements and ECMWF analyses during summer at Dome C, Antarctica. *Journal of Geophysical Research*, 115(D05104): doi http://dx.doi.org/10.1029/2009JD012741.

Girard, E., and Blanchet, J. P., 2001: Simulation of arctic diamond dust, ice fog, and thin stratus using an explicit aerosol-cloud-radiation model. *Journal of the Atmospheric Sciences*, 58(10): 1199–1221.

Gobiet, A., 2005: Climatological validation of stratospheric temperatures in ECMWF operational analyses with CHAMP radio occultation data. *Geophysical Research Letters*, 32(L12806): doi http://dx.doi.org/10.1029/2005GL022617.

Guo, Z. C., Bromwich, D. H., and Cassano, J. J., 2003: Evaluation of polar MM5 simulations of Antarctic atmospheric circulation. *Monthly Weather Review*, 131(2): 384–411.

IPCC, 2012: Special report of the IPCC (Managing the risks of extreme events and disasters to advance climate change adaptation). Cambridge, U.K.: Cambridge University Press, 1–20.

IPCC, 2013: Summary for Policymakers of Climate Change 2013: the Physical Science Basis. Contribution of Working Group I to the Fifth Assessment Report of the Intergovernmental Panel on Climate Change. Cambridge, U.K.: Cambridge University Press, 1–33.

Johanson, C. M. and Fu, Q., 2007: Antarctic atmospheric temperature trend patterns from satellite observations. *Geophysical Research Letters*, 34(12): L12703, doi http://dx.doi.org/10.1029/2006GL029108.

Kalnay, E., Kanamitsu, E. M., Kistler, R., Collins, W., Deaven, D., Gandin, L., Iredell, M., Saha, S., White, G., Woollen, J., Zhu, y., Chelliah, M., Ebisuzaki, W., Hiiggins, W., Janowiak, J., Mo, K. C., Ropelewski, C., Wang, J., Leetmaa, A., Reynolds, R., Jenne, R., and Joseph, D., 1996: The NCEP-NCAR 40-year reanalysis project. *Bulletin of the American Meteorological Society*, 77(3): 437–471.

Kennicutt, M. C., Chown, S. L., Cassano, J. J., Liggett, D., Massom, R., Peck, L. S., Rintoul, S. R., Storey, J. W. V., Vaughan, D. G., Wilson, T. J. and Sutherland, W. J., 2014: Six priorities for Antarctic science. *Nature Climate Change*, 512: 23–25.

Kharin, V. V., Zwiers, F. W., Zhang, X., and Hegerl, G. C., 2007: Changes in temperature and precipitation extremes in the IPCC ensemble of global coupled model simulations. *Journal of Climate*, 20(8): 1419–1444.

Kistler, R., Kalnay, E., Collins, W., Saha, S., White, G., Woolen, J., Chelliah, M., Ebisuzaki, W., Kanamitsu, M., Kousky, V., Dool, H. v.d., Jenne, R., and Fiorino, M., 2001: The NCEP-NCAR 50-year reanalysis: monthly means CD-ROM and documentation. *Bulletin of the American Meteorological Society*, 82(2): 247–267.

Lachlan-Cope, T., 2010: Antarctic clouds. *Polar Research*, 29(2): 150–158.

Ma, Y., Bian, L., Xiao, C., and Allison, I., 2008: Correction of snow accumulation impacted on air temperature from automatic weather station on the Antarctic ice sheet. *Chinese Journal of Polar Research*, 20(4): 299–309.

Marshall, G. J., and Thompson, D. W. J., 2016: The signatures of large-scale patterns of atmospheric variability in Antarctic surface temperatures. *Journal of Geophysical Research–Atmospheres*, 121(7): 3276–3289.

Moore, G. W. K., 2004: High Himalayan meteorology: weather at the South Col of Mount Everest. *Geophysical Research Letters*, 31(L18109): doi http://dx.doi.org/10.1029/2004GL020621.

Moore, G. W. K., and Semple, J. L., 2006: Weather and death on Mount Everest: an analysis of the into thin air storm. *Bulletin of the American Meteorological Society*, 87(4): 465–480.

Morrison, H., Pinto, J. O., Curry, J. A., and McFarquhar, G. M., 2008: Sensitivity of modeled arctic mixed-phase stratocumulus to cloud condensation and ice nuclei over regionally varying surface conditions. *Journal of Geophysical Research–Atmospheres*, 113(D5): doi http://dx.doi.org/10.1029/2007JD008729.

Pezza, A. B., Rashid, H. A., and Simmonds, I., 2012: Climate links and recent extremes in antarctic sea ice, high-latitude cyclones, Southern Annular Mode and ENSO. *Climate Dynamics*, 38(1-2): 57–73.

Poli, P., Healy, S. B., and Dee, D. P., 2010: Assimilation of global positioning system radio occultation data in the ECMWF ERA-Interim reanalysis. *Quarterly Journal of the Royal Meteorological Society*, 136(653): 1972–1990.

Qin, D., Zhang, J., Shan, C., and Song, L., 2015: *China National Assessment Report on Risk Management and Adaptation of Climate Extremes and Disasters*. China: Science Press, 124 pp.

Russo, S., Dosio, A., Graversen, R. G., Sillmann, J., Carrao, H., Dunbar, M. B., Singleton, A., Montagna, P., Barbola, P., and Vogt, J. V., 2014: Magnitude of extreme heat waves in present climate and their projection in a warming world. *Journal of Geophysical Research: Atmospheres*, 119(22): 12500–12512.

Scambos, T. A., Bohlander, J. A., Shuman, C. A., and Skvarca, P., 2004: Glacier acceleration and thinning after ice shelf collapse in the Larsen B embayment, Antarctica. *Geophysical Research Letters*, 31(18): http://dx.doi.org/10.1029/2004GL020670.

Shepherd, A., Ivins, E. R., Geruo, A., Barletta, V. R., Bentley, M. J., Bettadpur, S., Briggs, K. H., Bromwich, D. H., Forsberg, R., Galin, N., Horwath, M., Jacobs, S., Joughin, I., King, M. A., Lenaerts, J. T., Li, J., Ligtenberg, S. R., Luckman, A., Luthcke, S. B., McMillan, M., Meister, R., Milne, G., Mouginot, J., Muir, A., Nicolas, J. P., Paden, J., Payne, A. J., Pritchard, H., Rignot, E., Rott, H., Sorensen, L. S., Scambos, T. A., Scheuchl, B., Schrama, E. J., Smith, B., Sundal, A. V., van Angelen, J. H., van de Berg, W. J., van den Broeke, M. R., Vaughan, D. G., Velicogna, I., Wahr, J., Whitehouse, P. L., Wingham, D. J., Yi, D., Young, D., and Zwally, H. J., 2012: A reconciled estimate of ice-sheet mass balance. *Science*, 338(6111): 1183–1189.

Simmons, A. J., 2004: Comparison of trends and low-frequency variability in CRU, ERA-40, and NCEP/NCAR analyses of surface air temperature. *Journal of Geophysical Research*, 109: D24115, doi http://dx.doi.org/10.1029/2004JD005306.

Simmons, A. J., Poli, P., Dee, D. P., Berrisford, P., Hersbach, H., Kobayashi, S., and Peubey, C., 2014: Estimating low-frequency variability and trends in atmospheric temperature using ERA-Interim. *Quarterly Journal of the Royal Meteorological Society*, 140(679): 329–353.

Taylor, K. E., 2001: Summarizing multiple aspects of model performance in a single diagram. *Journal of Geophysical Research*, 106: 7183–7192.

Uppala, S. M., Kållberg, P. W., Simmons, A. J., Andrae, U., Bechtold, V. D. C., Fiorino, M., Gibson, J. K., Haseler, J., Hernandez, A., Kelly, G. A., Li, X., Onogi, K., Saarinen, S., Sokka, N., Allan, R. P., Andersson, E., Arpe, K., Balmaseda, M. A., Beljaars, A. C. M., Berg, L. V. D., Bidlot, J., Bormann, N., Caires, S., Chevallier, F., Dethof, A., Dragosavac, M., Fisher, M., Fuentes, M., Hagemann, S., Hólm, E., Hoskins, B. J., Isaksen, L., Janssen, P. A. E. M., Jenne, R., McNally, A. P., Mahfouf, J. F., Morcrette, J. J., Rayner, N. A., Saunders, R. W., Simon, P., Sterl, A., Trenberth, K. E., Untch, A., Vasiljevic, D., Viterbo, P., and Woollen, J., 2005: The ERA-40 re-analysis. *Quarterly Journal of the Royal Meteorological Society*, 131(612): 2961–3012.

Van de Berg, W. J., Van den Broeke, M. R., and Van Meijgaard, E., 2007: Heat budget of the East Antarctic lower atmosphere derived from a regional atmospheric climate model. *Journal of Geophysical Research*, 112(D23): doi http://dx.doi.org/10.1029/2007JD008613.

Van Den Broeke, M. R., 1998: The semi-annual oscillation and Antarctic climate. Part 1: influence on near surface temperatures (1957–79). *Antarctic Science*, 10(02): 175–183.

van den Broeke, M. R., Winther, J. G., Isaksson, E., Pinglot, J. F., Karlof, L., Eiken, T., and Conrads, L., 1999: Climate

variables along a traverse line in Dronning Maud Land, East Antarctica. *Journal of Glaciology*, 45(150): 295–302.

Van Wessem, J. M., Reijmer, C. H., Lenaerts, J. T. M., Van de Berg, W. J., Van den Broeke, M. R., and Van Meijgaard, E., 2014: Updated cloud physics in a regional atmospheric climate model improves the modelled surface energy balance of Antarctica. *The Cryosphere*, 8(1): 125–135.

Wang, A., and Zeng, X., 2012: Evaluation of multireanalysis products with in situ observations over the Tibetan Plateau. *Journal of Geophysical Research*, 117(D5): doi http://dx.doi.org/10.1029/2011JD016553.

Wilson, A. B., Bromwich, D. H., and Hines, K. M., 2012: Evaluation of Polar WRF forecasts on the Arctic System Reanalysis Domain: 2. Atmospheric hydrologic cycle. *Journal of Geophysical Research–Atmospheres*, 117: doi http://dx.doi.org/10.1029/2011JD016765.

Xiao, C., Li, Y., Hou, S., Allison, I., Bian, L., and Ren, J., 2008: Preliminary evidence indicating Dome A (Antarctica) satisfying preconditions for drilling the oldest ice core. *Chinese Science Bulletin*, 53(1): 102–106.

Xie, A., Allison, I., Xiao, C., Wang, S., Ren, J., and Qin, D., 2014: Assessment of air temperatures from different meteorological reanalyses for the East Antarctic region between Zhonshan and Dome A. *Science China Earth Sciences*, 57(7): 1538–1550.

You, Q., Kang, S., Aguilar, E., Pepin, N., Flügel, W.-A., Yan, Y., Xu, Y., Zhang, Y., and Huang, J., 2010: Changes in daily climate extremes in China and their connection to the large scale atmospheric circulation during 1961–2003. *Climate Dynamics*, 36(11-12): 2399–2417.

You, Q., Min, J., Fraedrich, K., Zhang, W., Kang, S., Zhang, L., and Meng, X., 2014: Projected trends in mean, maximum, and minimum surface temperature in China from simulations. *Global and Planetary Change*, 112: 53–63.

Zhang, S. E. D., Wang, Z., Zhou, C., and Shen, Q., 2007: Surface topography around the summit of Dome A, Antarctica, from real-time kinematic GPS. *Journal of Glaciology*, 53: 159–160.

Zhao, T., Guo, W., and Fu, C., 2008: Calibrating and evaluating reanalysis surface temperature error by topographic correction. *Journal of Climate*, 21(6): 1440–1446.

MS submitted 28 July 2015
MS accepted 14 July 2016